Available online at www.sciencedirect.com
SCIENCE DIRECT®
Carbon 43 (2005) 970–977
CARBON
www.elsevier.com/locate/carbon

Diameter and morphology dependence on experimental conditions of carbon nanotube arrays grown by spray pyrolysis

L. Tapasztó [a,*], K. Kertész [a], Z. Vértesy [a], Z.E. Horváth [a], A.A. Koós [a], Z. Osváth [a], Zs. Sárközi [b], Al. Darabont [b], L.P. Biró [a]

[a] *Research Institute for Technical Physics and Materials Sciences, Nanotechnology Department, Konkoly Teghe 29-33, H-1525, P.O. Box 49, 1121 Budapest, Hungary*
[b] *Faculty of Physics, "Babes-Bolyai" University, Str M. Kogalniceanu No. 1, R-3400, Cluj-Napoca, Romania*

Received 4 February 2004; accepted 15 November 2004
Available online 25 January 2005

Abstract

A systematic study on the controlled growth of large areas of aligned multi-wall carbon nanotube arrays, from ferrocene–benzene precursor, and of nanotube junctions from ferrocene–thiophene precursor, without hydrogen addition, using an injection CVD method easy to scale up for industrial production is reported.

A detailed study is presented of how the synthesis parameters such as growth temperature, active solution flow rate, catalyst concentration or sulfur addition can control the properties and morphology of the grown nanotube mat. Nanotube junctions with considerable yield can be grown with our method by adding sulfur to the synthesis process. The sulfur addition also results in growth of carbon nanocones (CNC) in the lower temperature regime of the furnace. Observation of single-wall carbon nanotubes in our STM investigations provides further indication that under properly chosen conditions SWCNTs can be grown with similar continuous processes.

Keywords: Carbon nanotubes; Chemical vapor deposition, Pyrolysis; Scanning tunneling microscopy, Transmission electron microscopy

1. Introduction

In recent years increasing attention has been focused on controlling the growth of aligned nanotube arrays of desired morphologies dimensions and properties [1,2]. Arrays of well-aligned carbon nanotubes over large areas are prerequisites for the realization of many applications, the best known of them being field emission devices [3]. Recently such arrays have been successfully applied as sensors [4]. On the other hand the synthesis of nanotube junctions is important because of the role they could play in future electronics where multi-terminal devices are needed for higher integration levels [5].

Synthesis of nanotubes by CVD methods proved to be more controllable and more cost efficient than the high temperature methods, such as arc discharge or laser ablation. A further advantage is that often CVD growth apparatus can be operated at atmospheric pressure and temperatures in the range of 500–1000 °C, without using of hazardous gases like CO. However, the reduction of catalyst activity and selectivity, after certain reaction time, leads to the deposition of amorphous carbon.

The synthesis of aligned multi-walled carbon nanotubes by catalytic pyrolysis of hydrocarbons using a simple and inexpensive method, which can be easily scaled up for continuous or semi-continuous production, has been reported by many authors [6–12].

The main advantage of the injection CVD methods is that they do not require preformed substrates, the

* Corresponding author. Tel.: +36 1 392 2526; fax: +36 1 392 2226.
E-mail address: tapaszto@mfa.kfki.hu (L. Tapasztó).

0008-6223/$ - see front matter © 2004 Elsevier Ltd. All rights reserved.
doi:10.1016/j.carbon.2004.11.048

catalyst particles are continuously supplied thus the deactivation process does not lead inevitably to the cessation of the growth process, making possible the continuous production of nanotubes.

In this paper we present a systematic study on the effects of synthesis parameters such as growth temperature, catalyst concentration and active solution flow rate, on the properties of the as-grown aligned nanotube fields using an injection CVD method with a ferrocene–benzene solution as catalyst, respectively carbon source.

The synthesis of nanotube junctions in various CVD processes has been also reported previously [13,14]. Because of their potential industrial application in nanoelectronics or in material reinforcement, it is desirable to synthesize nanotube junctions by continuous processes without further addition of hazardous materials such as hydrogen. This paper also reports a method for growth of nanotube junctions by an injection CVD process without hydrogen addition.

Another desirable development is to adapt this method to the production of single-wall nanotubes. Cheng et al. [15] reported the production of bundles of aligned SWCNT in a semi-continuous process, but their experimental finding seems to be controversial as reported by the Rice university group [16]. More recently Vivekchand et al. reported the occurrence of SWCNT's in a similar process, but there is little direct evidence [17]. We here report the observation of single wall tubes and bundles of SWCNT's in STM measurements of samples grown by our injection CVD method.

2. Experimental

The experimental setup used in our experiments to synthesize aligned nanotube arrays and nanotube junctions consist of an electric furnace with an effective heating length of 200 mm, a quartz reactor of 18 mm inner diameter and a nozzle with two concentric tubes of 0.8 and 1.8 mm inner diameter, respectively [18]. The inner tube of the nozzle carries the active solution, while the outer one guides the carrier gas in order to pulverize the solution. The experimental setup is similar to that reported by Kamalakaran et al. [6]. In all the experiments 50 ml ferrocene–benzene or ferrocene–thiophene solution, with ferrocene concentration between 0.03 g/ml and 0.09 g/ml, was sprayed into the furnace, using argon as carrier gas. The carrier gas flow rate was 500 l/h in all the experiments. The active solution flow rate was varied between 30 ml/h and 180 ml/h. The furnace was preheated to a temperature between 800 and 1000 °C. No external source of hydrogen was used in our experiments. The ferrocene decomposes to provide the iron catalyst particles required for the nucleation of nanotubes, while benzene and thiophene are used as carbon and sulfur feedstock, respectively.

The aligned nanotube films grew on the quartz reactor wall, the tubes having a normal orientation to the reactor wall. The amount of material collected was typically in the range of tenth of grams from 50-ml active solution, and varied as a function of synthesis parameters. The highest yield was achieved at 875 °C, 180 ml/h active solution flow rate, 0.06 g/ml ferrocene concentration and 500 l/h carrier gas flow rate. TEM and SEM images proved that after optimizing the growth parameters, almost all of the grown material consists of large areas of well-aligned multi-wall carbon nanotubes (Fig. 1).

Several pyrolysis experiments were carried out, using different reaction conditions in order to optimize the synthesis parameters. The variation of growth parameters was done systematically to investigate the effects of parameters such as: temperature, ferrocene concentration, active solution flow rate, and the sulfur addition, on the properties of the grown aligned carbon nanotube material. The soot deposited on the walls of the quartz tube was collected and analyzed by transmission and scanning electron microscopy (TEM and SEM), X-ray diffraction, and scanning tunneling microscopy (STM).

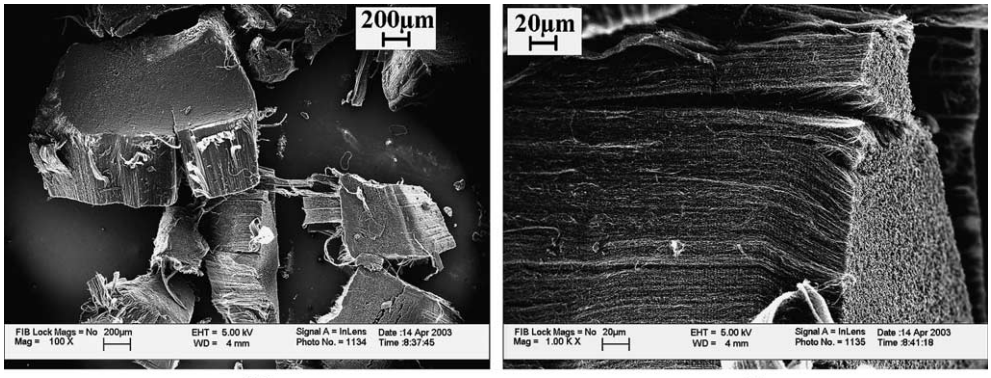

Fig. 1. SEM images of large areas of aligned nanotube films, grown at 875 °C, 180 ml/h active solution flow rate, 0.06 g/ml ferrocene concentration in benzene.

3. Results and discussion

3.1. Growth temperature

The 800–950 °C temperature window was found to be suitable for growing nanotubes with a considerable yield. The diameter of the grown tubes depends strongly on the growth temperature; a decrease of average diameter with increasing temperature was found. From the TEM measurements we were able to determine the diameter distribution for the samples grown at different temperatures. As shown in Fig. 2, the average diameter decreases with increasing temperature.

In the lower temperature range, the average tube diameter is expected to increase with temperature [19]. In the relatively high temperature regime of our experiments (above 850 °C) we observed the decrease of the average diameter of the nanotubes with increasing temperature in agreement with findings of Singh et al. [19] for a different precursor and experimental setup.

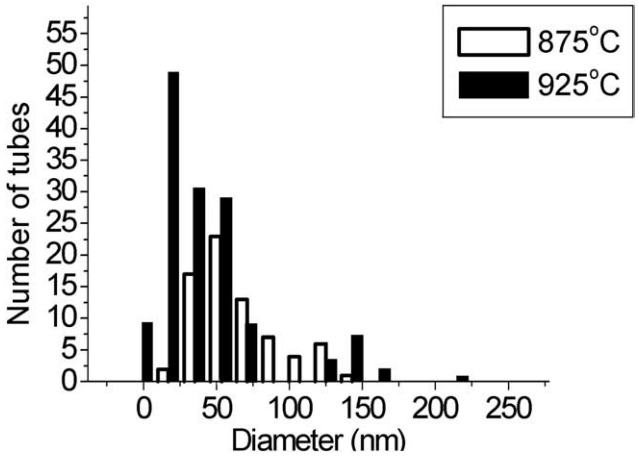

Fig. 2. The diameter distribution of the nanotube samples grown at 875 °C (light bars) and 925 °C (dark bars) indicating a decreasing average diameter with increasing synthesis temperature. Both samples grown with 0.06 g/ml ferrocene concentration and 60 ml/h solution flow rate.

We attribute the decrease of the average diameter to the increasing percentage of the small diameter tubes in the sample. The origin of this process might be the continuous catalyst injection during the growth. At the beginning of the synthesis process, the catalyst particles reach the substrate and due to diffusion begin to form catalyst clusters from which the nanotubes are growing with diameters strongly correlated to the size of the catalyst clusters [20]. Hence at higher temperatures, nanotubes with higher diameters are expected to grow, due to the increasing mobility of the iron particles on the quartz surface, which leads to the formation of larger clusters. [19]. Once the nanotube field starts to grow, the incoming catalyst particles cannot reach the substrate, and they will be deposited on the growing nanotube mat. Catalyst cluster formation may also take place on the external surface of the already growing nanotubes, generating nucleation sites for smaller diameter CNT's in some cases SWCNT's, and leading to a bimodal diameter distribution of the samples. The temperature may have an important role in the catalyst cluster formation, on the nanotube mat as well; however the precise mechanism has to be clarified.

The bimodal diameter distribution was frequently observed clearly both from SEM and TEM measurements. The SEM micrographs in Fig. 3 shows the presence of the thin nanotubes with approximately 20 nm average outer diameter besides large nanotubes with a 60 nm average diameter. In the as-grown material, the larger (60 nm) diameter tubes are aligned while the smaller diameter tubes are entangled.

The bimodal diameter distribution obtained from the TEM and SEM images of the above sample is represented quantitatively in the diagram in Fig. 4.

This bimodal diameter distribution at high temperatures was described by Sing et al. [19]. They found the bimodal distribution to disappear at lower tempera-

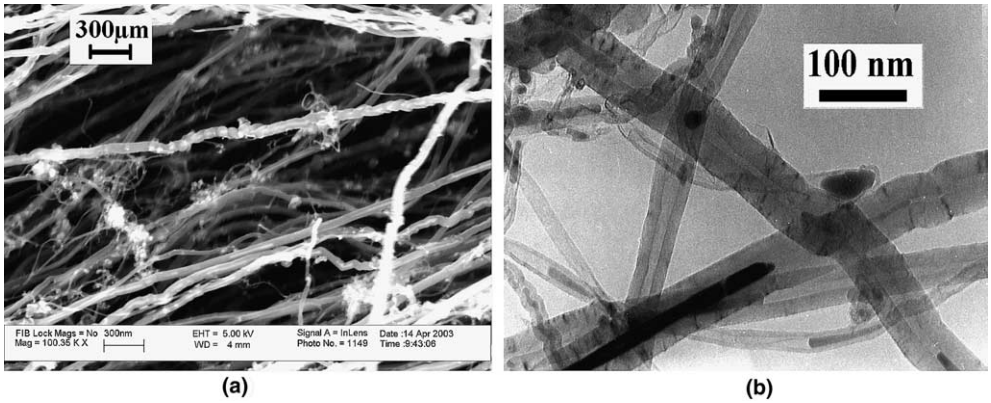

Fig. 3. SEM (left) and TEM (right) image of the nanotubes grown at 875 °C showing the bimodal diameter distribution with large nanotubes of 60 nm average diameter, and smaller ones with 20 nm average diameter.

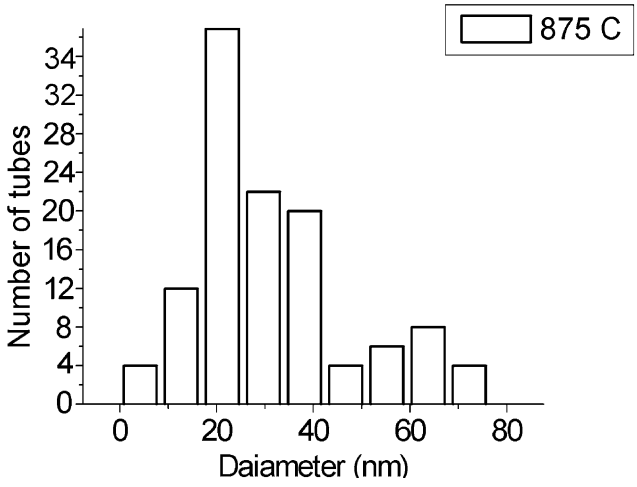

Fig. 4. The diameter distribution diagram of the sample grown at 875 °C, 180 ml/h active solution flow rate, 0.06 g/ml ferrocene concentration in benzene.

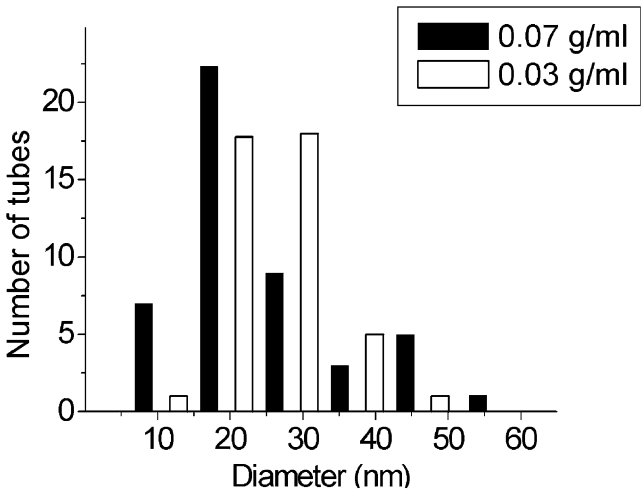

Fig. 5. Diameter distribution diagram of samples grown at ferrocene concentrations of 0.07 g/ml and 0.03 g/ml ferrocene in benzene. The growth temperature was 875 °C in both cases. The bimodal diameter distribution disappears at the lower ferrocene concentration.

tures, where the temperature dependence of the diameter becomes "normal" too, which is in good agreement with our explanation.

An interesting and potentially useful characteristic of these aligned nanotubes is the filling of the tubes hollow core with catalyst particles, forming nanowires of several hundreds of nanometers. From the TEM images presented in Fig. 3, one can note the partial filling for both larger and smaller diameter multi-wall nanotubes.

3.2. Ferrocene concentration

It is believed that the size of catalyst particles is strongly correlated with the diameter of the tube grown on it [20]. It should follow that the average diameter of the grown tubes decreases with decreasing ferrocene concentration [19]. In fact, in experiments, for a given nozzle and given flow rate the size of the iron particles may be related to two factors: the size of liquid droplets produced by nozzle and the ferrocene concentration of the solution. We found only a small variation (within measurement error) of tube diameter when decreasing the ferrocene concentration from 0.07 g/ml to 0.03 g/ml. The average diameter of the tubes was about 25 nm in both cases. At lower ferrocene concentration the bimodal distribution of diameters disappears, as shown in Fig. 5.

3.3. Ferrocene–benzene solution flow rate

In our experiments, we used relatively high flow rates of the ferrocene–benzene solution, up to 180 ml/h. With these high flow rates we were able to reach better yields and grow longer tubes than reported previously [19] with a similar method using considerably lower flow rates. With the sample grown with 180 ml/h active solution flow rate, at 875 °C temperature, 5×10^5 ml/h carrier gas flow rate, and 0.06 g/ml ferrocene in benzene, as active solution concentration, we reached the highest yield of 6.2 mg/cm^2 and the longest tubes near 500 μm, in our experiment (Fig. 1). The effect of active solution flow rate on diameter and the dispersion of diameters of the growing tubes are shown in Fig. 6.

By increasing the flow rate the average diameter decreases and also a narrower dispersion of diameters can be achieved (Fig. 6). The strong effect of flow rate on the average tube diameter must be related to the size of liquid droplets produced by the nozzle and the higher

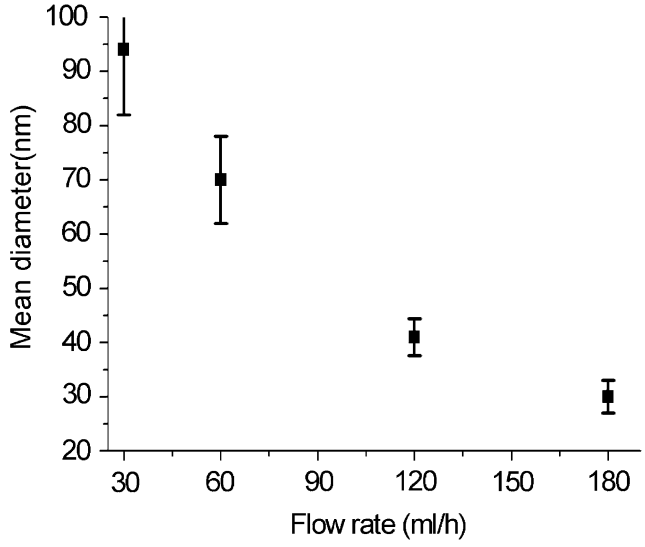

Fig. 6. Diameter dependence of carbon nanotubes from active solution flow rate, the bars indicate the magnitude (full width at half maximum) of the dispersion of diameters at 0.06 g/ml ferrocene concentration.

number of catalyst particles. The shorter duration time of the growth cycle for larger flow rates may also have a contribution, due to the uncatalysed thermal decomposition of benzene at high temperatures. This process may lead to the pyrolytic overcoating of the nanotubes. The alignment of tubes also can be improved by increasing the flow rate of the active solution.

3.4. Sulfur addition

To investigate the effect of sulfur addition on the synthesis process we replaced the benzene from the active solution with thiophene. We observed, by TEM and SEM investigations of the samples, the formation of L and Y carbon nanotube junctions with a considerable yield (Figs. 7 and 8). As can be seen on the SEM image in Fig. 8, the alignment of nanotubes is lost when benzene is replaced by thiophene.

Note that in our experiments we did not use additional hydrogen, formerly thought to be essential [13] in the formation of nanotube junctions. Beside the nanotube junctions, a large quantity of perfectly straight nanotubes was grown. The inner core of these straight tubes frequently was continuously filled with the catalyst material (Fig. 7a). This indicates that the presence of sulfur may facilitate the filling of tubes. The average diameter of these straight nanotubes was about 25 nm. Surprisingly, we observed that the dispersion of diameter distribution becomes appreciably narrower by replacing the benzene with thiophene (Fig. 9). Another peculiar characteristic of these tubes is that they always have open ends.

For the experiments with sulfur addition, the TEM investigation of the soot deposited on the wall of the quartz reactor in the lower temperature regions of the furnace (near the outlet and outside) shows a large number of hexagonal shape particles with dimensions between 50–100 nm. These hexagonal shape particles act as catalysts for short (50–100 nm), conically shaped carbon nanostructures (Fig. 10a).

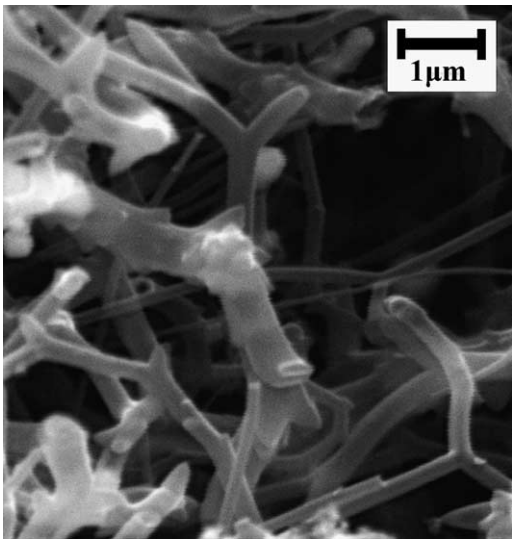

Fig. 8. SEM image showing a significant yield of carbon nanotube junctions, in the samples grown at 875 °C, 60 ml/h active solution flow rate and 0.06 g/ml solution of ferrocene in thiophene.

The experimentally found apex angles of the cones, varies between 35° and 40°. This is in good agreement with structural calculations using the pentagon defect model [21]. By considering four fused pentagons, incorporated in a hexagonal graphene sheet, the structure optimization results in a conical structure, with an apex

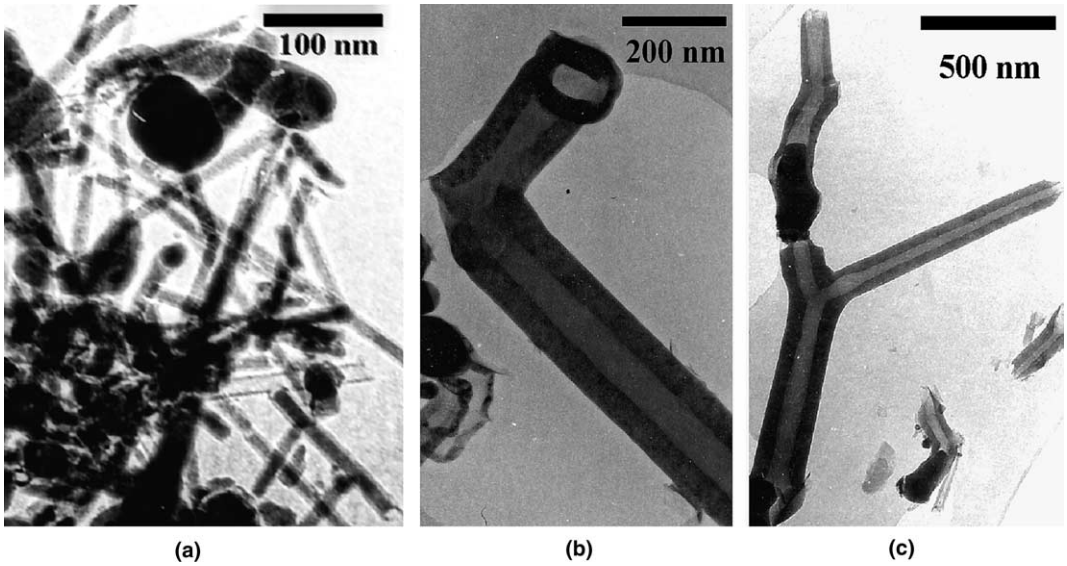

Fig. 7. TEM images of (a) straight CNTs continuously filled with catalyst particles; (b) L carbon nanotube junction; (c) Y branched carbon nanotube. All of them grown at 875 °C, 60 ml/h active solution flow rate and 0.06 g/ml solution of ferrocene in thiophene.

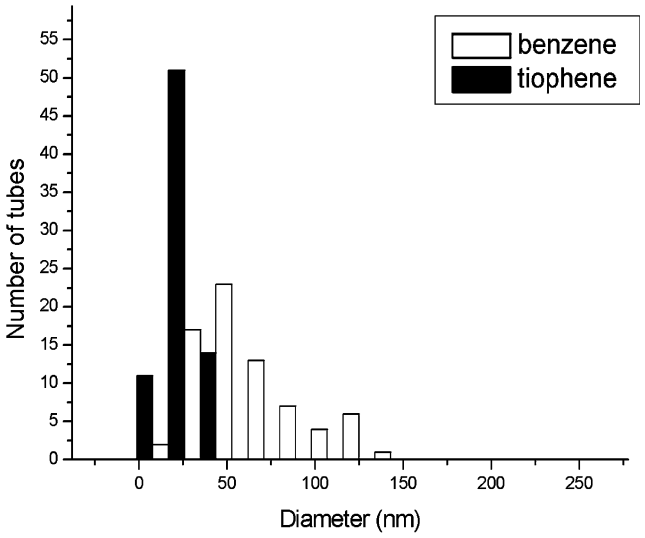

Fig. 9. Diameter distributions diagrams for nanotubes grown from benzene/ferrocene, respectively thiophene/ferrocene precursor. All the other growth parameters are the same for the two samples.

angle of 38.9° (Fig. 10b). It is tempting to assume the pentagon formation to the effect of sulfur addition in the same way as sulfur facilitates the incorporation of non-hexagonal rings in the process of nanotube junction formation.

3.5. Occurrence of SWCNT's

The STM investigation of the samples revealed, beside MWNT's with characteristic diameters (20–80 nm), the presence of nanotubes with diameters in the range typical for single-wall carbon nanotubes. Bundles of single-wall nanotubes were observed too. It is well known that it is not straightforward to decide from diameters measured by STM whether a nanotube is single wall or not, we can only estimate the tube diameter. On the other hand, it is sure, that the real tube diameter is somewhat larger than that measured form the apparent height in the STM image [22]. In Fig. 11a the STM image of a carbon nanotube is shown with an apparent diameter of 1.13 nm—as measured from the apparent height—lying on the HOPG substrate used as support for the STM measurements. The two mono-atomic steps in the HOPG layer, shown in the STM image, with apparent height about 0.3 nm, which is in good agreement with the 0.335 nm interlayer spacing in graphite, were used to check the height calibration of the STM.

Singh's group found the signature of SWCNT's in the Raman spectrum obtained from the top surface of the aligned films growth at high temperatures. They attribute the growth of SWCNT's to the formation of fine particles on top of the nanotube films [19]. These particles are supposed to act as nucleation sites for SWCNT's, which is in agreement with our proposal of the growth mechanism at high temperatures, leading to bimodal diameter distribution. As reported by many authors [19,23] the Raman spectrum obtained from the samples in similar experiments, clearly indicates the presence of the SWCNT's through the appearance of the radial breathing mode. TEM measurements could not unambiguously verify the presence of SWCNT's. This might be attributed to the attachment of the SWCNT's to the larger MWCNTs during the ultrasonication applied in sample preparation for TEM measurements.

As mentioned above, during STM investigation, we found also bundles of SWCNT's in our samples. Bundle formation is characteristic for the growth of SWCNT's. Following the bundles along the axis with the STM tip in some cases, we observed the splitting of the bundle into branches, as can be seen in the 3D STM image in Fig. 11b.

Cheng et al. [23] reported the growth of SWCNT bundles with a similar procedure. A peculiar characteristic of these bundles was that they have a roughly round

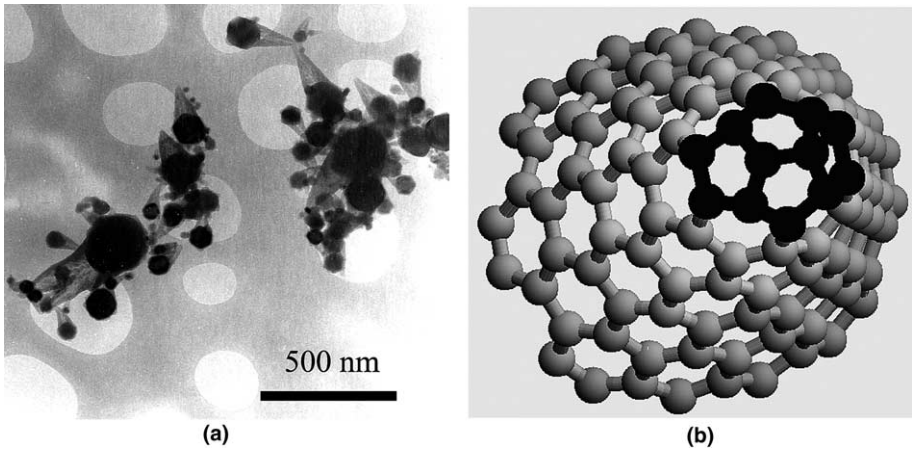

Fig. 10. (a) Carbon nanocones growing in experiments with sulfur addition on hexagonal shape catalyst particles in low temperature region, near the outlet of the furnace; (b) structural model of CNC's with four incorporated pentagons.

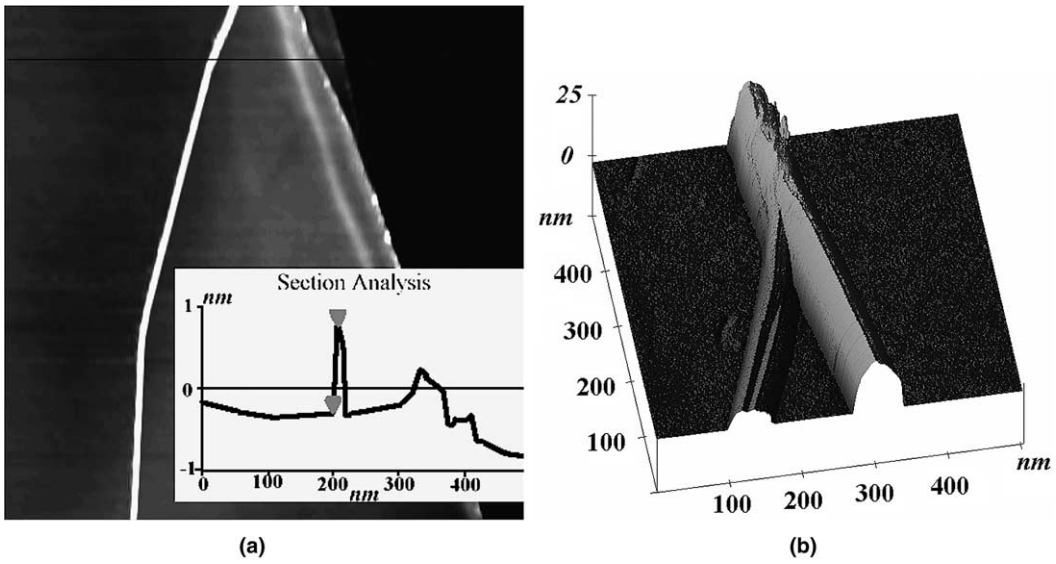

Fig. 11. (a) STM image of a single-wall carbon nanotube with 1.13 nm apparent diameter on HOPG showing two mono-atomic step of apparent height of 0.3 nm; (b) 3D STM image of a branching bundle of single-wall carbon nanotubes, both found in the sample grown at 875 °C, 60 ml/h flow rate, 0.06 g/ml ferrocene solution in benzene.

rope-like shape with some small bundles or single nanotubes split off from the larger ropes. We believe that in our STM measurements we have seen these branching bundles of SWCNT's. In order to increase the percentage of the SWCNT's present in the samples further optimization is needed in this direction.

4. Conclusions

Films of large size aligned multi-walled carbon nanotubes reaching 500 μm in length were grown on quartz substrates by spray pyrolysis of the solution of ferrocene in benzene. A systematic variation of growth parameters was done and their effect was studied. With a benzene–ferrocene solution and high active solution flow rates we reached higher yields, up to 6.2 mg/cm^2, and longer tubes (up to 500 μm) than reported previously with a similar method optimized for the ferrocene–toluene precursor [19]. It is shown that the diameter of the tubes decreases with increasing active solution flow rate, and it is confirmed the decrease of the diameter with increasing temperature in the range of high temperatures (above 850 °C), a possible explanation of this inverse diameter dependence based on the bimodal diameter distribution growth mechanism is given. The effect of sulfur addition on the synthesis was investigated, and the growth of nanotube junctions, like nanoknees, Y carbon nanotube junctions, without further hydrogen addition, is reported. The use of thiophene instead of benzene yields a significantly narrower diameter distribution for the straight nanotubes and a higher degree of filling with the catalyst material. The formation of carbon nanocones in an injection CVD method with sulfur addition is reported. Experimental results, supporting the pentagon defect model of carbon nanocones, are presented. This paper also provides new indication from STM measurements that SWCNT's are grown together with aligned MWNT in a continuous process. Further investigations are needed to optimize the process in this direction.

Acknowledgment

The work in Romania was supported by the Sapientia Research Programs Institute in the framework of fellowship 822/2001-K/513/2003.03.25, and in Hungary by OTKA through the grant no. T 043685. T.L. and K.K. gratefully acknowledge the support of Agora foundation.

References

[1] Mauron P, Emmenegger C, Zuttel A, Nutzenadel C, Sudan P, Schlapbach L. Synthesis of oriented nanotube films by chemical vapor deposition. Carbon 2002;40(8):1339–44.
[2] Siegal MP, Overmyer DL, Kottenstette RJ, Tallant DR, Yelton WG. Nanoporous-carbon films for microsensor preconcentrators. Appl Phys Lett 2002;80(21):3940–2.
[3] Choi YS, Cho YS, Kang JH, Kim YJ, Kim IH, Park SH, et al. A field-emission display with a self-focus cathode electrode. Appl Phys Lett 2003;82(20):3565–7.
[4] Modi A, Koratkar N, Lass E, Wei BQ, Ajayan PM. Miniaturized gas ionization sensors using carbon nanotubes. Nature 2003;424(6945):171–4.
[5] Meunier V, Nardelli MB, Bernholc J, Zacharia T, Charlier JC. Intrinsic electron transport properties of carbon nanotube Y-junctions. Appl Phys Lett 2002;81(27):5234–6.

[6] Kamalakaran R, Terrones M, Seeger T, Kohler-Redlich P, Ruhle M, Kim YA, et al. Synthesis of thick and crystalline nanotube arrays by spray pyrolysis. Appl Phys Lett 2000;77(21): 3385–7.
[7] Singh C, Shaffer MSP, Koziol KKK, Kinloch IA, Windle AH. Towards the production of large-scale aligned carbon nanotubes. Chem Phys Lett 2003;372(5–6):860–5.
[8] Andrews R, Jacques D, Rao AM, Derbyshire F, Qian D, Fan X, et al. Continuous production of aligned carbon nanotubes: a step closer to commercial realization. Chem Phys Lett 1999;303 (5–6):467–74.
[9] Lee YT, Kim NS, Park J, Han JB, Choi YS, Ryu H, et al. Temperature-dependent growth of carbon nanotubes by pyrolysis of ferrocene and acetylene in the range between 700 and 1000 °C. Chem Phys Lett 2003;372(5–6):853–9.
[10] Singh C, Shaffer MSP, Kinloch IA, Windle AH. Production of aligned carbon nanotubes by the CVD injection method. Physics B 2002;323(1–4):339–40.
[11] Mayne M, Grobert N, Terrones M, Kamalakaran R, Ruhle M, Kroto HW, et al. Pyrolytic production of aligned carbon nanotubes from homogeneously dispersed benzene-based aerosols. Chem Phys Lett 2001;338(2–3):101–7.
[12] Zhang X, Cao A, Wei B, Li Y, Wei J, et al. Rapid growth of well aligned carbon nanotube arrays. Chem Phys Lett 2002;362: 285–90.
[13] Deepak FL, Govindaraj A, Rao CNR. Synthetic strategies for Y-junction carbon nanotubes. Chem Phys Lett 2001;345(1–2):5–10.
[14] Satishkumar BC, Thomas PJ, Govindaraj A, Rao CNR. Y-junction carbon nanotubes. Appl Phys Lett 2000;77(16):2530–2.
[15] Cheng HM, Li F, Sun X, Brown SDM, Pimenta MA, Marucci A, et al. Bulk morphology and diameter distribution of single-walled carbon nanotubes synthesized by catalytic decomposition of hydrocarbons. Chem Phys Lett 1998;289(5–6):602–10.
[16] Jacoby M. Nanotube coils, story unfold. Chem and Eng News 1999;77:31.
[17] Vivekchand SRC, Cele LM, Deepak FL, Raju AR, Govindaraj A. Carbon nanotubes by nebulized spray pyrolysis. Chem Phys Lett 2004;386:313–8.
[18] Biro LP, Horvath ZE, Koos AA, Osvath Z, Vertesy Z, Darabont A, et al. Direct Synthesis of multi-walled and single-walled carbon nanotubes by spray-pyrolysis. J Optoelectron Adv Mater 2003;5:661–6.
[19] Singh C, Shaffer MS, Windle AH. Production of controlled architectures of aligned carbon nanotubes by an injection chemical vapour deposition method. Carbon 2003;41(2): 359–68.
[20] Cheung CL, Kurtz A, Park H, Lieber CM. Diameter-controlled synthesis of carbon nanotubes. J Phys Chem B 2002;106(10): 2429–33.
[21] Jaszczak JA, Robinson GW, Dimovski S, Gogotsi Y. Naturally occurring graphite cones. Carbon 2003;41:2085–92.
[22] Mark GI, Biro LP, Gyulai J. Simulation of STM images of three-dimensional surfaces and comparison with experimental data: carbon nanotubes. Phys Rev B 1998;58(19):12645–8.
[23] Cheng HM, Li F, Su G, Pan HY, He LL, Sun X, et al. Large-scale and low-cost synthesis of single-walled carbon nanotubes by the catalytic pyrolysis of hydrocarbons. Appl Phys Lett 1998;72(25):3282–4.